



**HAL**  
open science

# A Graph Neural Network with Spatio-temporal Attention for Multi-sources Time Series Data: An application to Frost Forecast

Hernan Lira, Luis Martí, Nayat Sanchez-Pi

► **To cite this version:**

Hernan Lira, Luis Martí, Nayat Sanchez-Pi. A Graph Neural Network with Spatio-temporal Attention for Multi-sources Time Series Data: An application to Frost Forecast. *Sensors*, 2022, 22 (4), pp.1486. 10.3390/s22041486 . hal-03541565v1

**HAL Id: hal-03541565**

**<https://inria.hal.science/hal-03541565v1>**

Submitted on 24 Jan 2022 (v1), last revised 15 Feb 2022 (v2)

**HAL** is a multi-disciplinary open access archive for the deposit and dissemination of scientific research documents, whether they are published or not. The documents may come from teaching and research institutions in France or abroad, or from public or private research centers.

L'archive ouverte pluridisciplinaire **HAL**, est destinée au dépôt et à la diffusion de documents scientifiques de niveau recherche, publiés ou non, émanant des établissements d'enseignement et de recherche français ou étrangers, des laboratoires publics ou privés.



Distributed under a Creative Commons Attribution 4.0 International License

# A Graph Neural Network with Spatio-temporal Attention for Multi-sources Time Series Data: An application to Frost Forecast

Hernan Lira<sup>ID\*</sup>, Luis Martí<sup>ID</sup>, and Nayat Sanchez-Pi<sup>ID</sup>

Inria Chile Research Center; {hernan.lira, luis.marti, nayat.sanchez-pi}@inria.cl

\* Correspondence: [hernan.lira@inria.cl](mailto:hernan.lira@inria.cl).

**Abstract:** Frost forecast is an important issue in climate research because of its economic impact on several industries. In this study, we propose GRAFT-Frost, a graph neural network (GNN) with spatio-temporal architecture, which is used to predict minimum temperatures and the incidence of frost. We developed an IoT platform capable of acquiring weather data from an experimental site, in addition data was collected from 10 weather stations in close proximity to the aforementioned site. The model considers spatial and temporal relations while processing multiple time series simultaneously. Performing predictions of 6, 12, 24 and 48 hours in advance, this model outperforms classical time series forecasting methods including, linear and non-linear machine learning methods, simple deep learning architectures and non-graph deep learning models. In addition, we show that our model significantly improves on the current state of the art of frost forecasting methods.

**Keywords:** Frost forecasting; Graph Neural Networks; Spatio-temporal attention

---

## 1. Introduction

Generating accurate weather forecasts from reliable localized data is a key feature of precision agriculture that enables farmers to improve their resources in terms of efficiency, productivity, sustainability etc.. Moreover, it is a tool for countering weather uncertainty by reducing the risks posed by extreme weather that can impact the overall quality of the production. Frost is one such threat that kills plant tissue causing low production and economic losses since it prevents the usual development of crops. During some periods of the year temperatures can drop considerably between day and night, with temperatures reaching below freezing. A low temperature can cause the crop to flower early or if there is frost it can cause a considerable reduction in production [1]. These negative consequences could be prevented or mitigated with a frost forecast model that provides information to the farmer regarding the probability of a frost event several hours in advance, so the farmer can take action to protect the crops.

From a forecasting perspective, the prediction of frost events presents some challenges. For instance, they are a complex meteorological phenomenon influenced by a combination of environmental factors, — including air temperature, humidity, radiation, and wind, — and local factors — including topography and field orientation. Since there are local factors involved, frost events can occur in small areas even within the same crop field. [2]. Therefore, a method to collect high resolution weather data is required.

Typical weather data sources such as open weather, used for global weather forecasts, or national weather stations are useful to understand the weather dynamics across big areas. Previous research have used frost forecast models from these sources, but they are limited to forecasting in the vicinity of the weather station [3]. Therefore, these methods do not provide the resolution required when seeking to forecast the weather in a specific location/field. As a consequence, farmers use these forecasts as a reference, but most of their decisions to prevent frost events are based on experience and intuition.

To collect data specifically from a field we developed a low cost and easy-to-install IoT platform, with environmental sensors and cloud technologies for collecting and storing data. Specifically, we measure air temperature, air humidity and relevant metadata. In

addition, we use meteorological data collected from weather stations located near the field [4]. The purpose is to provide the farmer with relevant information so that they can make informed decisions. The frost forecasting model requires an intelligent component that uses field data to capture specific conditions about the field combined with weather stations data in order to capture weather dynamics and possible future scenarios.

The majority of research relating to frost forecasting is based on simulating partial differential equations or traditional statistical models in order to predict future weather conditions. [5]. This approach is computationally expensive as it requires a recurrent theoretical upgrade to incorporate weather and atmospheric assumptions. On the contrary, machine learning algorithms do not make any assumptions about weather behavior. Instead, they use historical weather data as an input and train a model to predict future weather values [3].

There are some challenges relating to machine learning models. Since frost can be highly variable across a small area, the collection of temperature data usually from weather stations is not available with sufficient frequency. In addition, the number of frost events during the year is relatively small making it difficult to build an accurate prediction model due to limited available data [2]. Finally, by viewing the model as a binary classification problem i.e. (Frost/No Frost) we needed to consider that both errors are unwanted. If no frost is predicted and the frost occurs, it may impact on the partial or total loss of production. On the contrary, if frost is predicted and the frost does not occur, unnecessary resources such as fuel and electricity used to mitigate the frost will be wasted.

In light of the aforementioned constraints especially the scarcity of data and small datasets, a range of machine learning models were evaluated, including models to learn time series data as well as advanced deep learning architectures. In particular, graph neural networks (GNN) and attention mechanisms were considered suitable for this problem since they incorporate spatial knowledge that can model field and environmental interactions [6,7]. In addition, since the occurrence of frost is caused by a prior movement of environmental factors, GNNs can be naturally extended to model this type of temporal interaction. Therefore, in this paper we discuss a time series forecasting problem using GNNs and attention.

In this study, we collected air temperature and humidity data from an experimental site and from 10 weather stations. In particular, we propose GRASST-Frost, a GNN with spatio-temporal attention architecture for frost forecast. We map weather stations' locations to nodes on a graph and construct the edges based on geographical proximity. Furthermore, the adjacency matrix is optimized during the training phase, therefore other interactions can be learned. We utilize spatio-temporal attention to incorporate similar locations and time.

To the best of our knowledge, deep learning and graph neural networks have so far not been applied to the frost forecasting problem. Although considerable research has been devoted to this area, most of the research has focused on developing an IoT platform for collecting in-place weather data. Consequently, little attention has been paid to developing a model that can take advantage of multiple data sources and spatio-temporal dynamics. However, GNN models have recently been adopted for traffic forecasting, epidemiology and fraud detection. The implementation of GNN models in these scenarios showed the potential for predicting multivariate time series [8,9] and graph attentional networks for capturing spatio-temporal dynamics citepcheng2020graph, li2021spatiotemporal, kong2020stgat.

Our contributions to this field are two-fold. First, we propose a full pipeline for the frost problem ranging from the development of an IoT platform, data collection and forecasting model using two data sources. Second, we approach the frost problem by proposing a multivariate time series forecasting method, GRASST-Frost, that computes each time series at the same time. This method is based on a graph data structure, and it uses a spatio-temporal attention mechanism for weighted relevance according to time and/or space.

Moreover, this paper seeks to answer the following research questions:

1. Is a graph neural network capable of improving the time series forecasting of data sources from different locations in comparison to state of the art frost forecasting methods?
2. Does the spatio-temporal attention mechanism improve forecasts?
3. Does the combined use of different data sources improve forecasts?

To answer the first question, we compare our approach with classical time series, machine learning and deep learning methods by classification and regression metrics, which are currently the state of the art for frost forecasting. With regards to the second question, we compare our approach with GNN models proposed in previous studies that do not use spatio-temporal attention mechanisms. For the final question we compare the forecasts using separate data sources.

The proposed model outperforms current state of the art methods for predicting temperature and classifying frost from 6 h, 12 h, 24 h and 48 h in advance. Furthermore, graph-based modeling and spatio-temporal attention mechanisms are key factors to perform a more accurate prediction and minimize classification errors.

The rest of the paper is organized into the following sections: Section 2 examines previous studies regarding machine learning for time series, weather and frost forecasting. Section 3 describes the platform and our proposed method. After that, Section 4 presents the experiments and results, and then we offer a discussion of the results in Section 5. Finally, Section 6 concludes the paper and presents possible directions for future work.

## 2. Related Work

Mort et al. [10] and Verdes et al. [11] are two research studies that address the frost phenomenon using machine learning. In these studies, the authors use artificial neural networks to create temperature prediction models based on weather time series data and apply them to agricultural applications. Their principal objectives are to predict the next day's minimum temperature using historical data. In recent years there have been great advances in the field of Internet of things (IoT) systems and Deep Learning. Thanks to these advancements it has been possible to install a wide variety of sensors and collect data from almost any place of interest with the purpose of building accurate prediction models. Regarding IoT systems designed for weather forecasting, Muck et al. [12] designed an IoT based weather station using a Raspberry Pi, which provides short-term weather forecasting. Similarly, Levin et al. [13] presents a weather forecasting system based on a Raspberry Pi 3 Model B+ with environmental sensors and a weather forecasting algorithm. Their systems monitor air temperature, humidity, pressure, and altitude at experimental locations. Their weather forecast algorithms are based on a Linear Regression Model. Other studies such as Diedrichs et al. [3] and Castaneda-Miranda et al. [14] used IoT devices to extract weather data from selected locations as well, but instead of focusing on weather, they used classic applied machine learning techniques to predict frost events. Likewise, the research group of Guillén-Navarro et al. [1,15] have developed over the years an IoT platform to predict frost events. This platform appears to be more robust than the previous studies in terms of engineering and technological components. Although these studies have made interesting progress in terms of IoT and sensor data collection systems, the development of their machine learning models have been limited. Therefore, the resulting prediction results are unsatisfactory in terms of error rates and/or classification metrics. In addition, the data sources have been constrained to the experimental field where the system is located.

Few studies have attempted to focus on the development of the frost forecast model itself. For example, Ding et al. [2] concentrated their efforts on the development of a causal-effect machine learning model that uses locally collected temperature, humidity and radiation data to create frost prediction. They were able to describe causal relationships between variables and outputs; however, their model requires improvements to minimize the false positive predictions. Another example is the study by Cadenas et al. [16], which is

based on a soft computing framework that collects and stores weather data. They propose a data preprocessing technique to build fuzzy time series from raw data and serve it as an input to classification and regression problems. In addition, Guillén-Navarro et al. [17] uses a simple Long short-term memory (LSTM) architecture to produce frost forecasts from data collected using their IoT system. Although these studies provide interesting methods to address the frost forecasting problem, there are still a large range of solutions to investigate. For example, exploring current developments within deep learning models that could improve forecasts and include different data sources.

In contrast to frost forecasting, weather-related forecasting has plenty of studies that use advanced deep learning techniques. For instance Shi et al. [18] proposed a fully connected convolutional LSTM network to predict short-term future rainfall intensity in a local area and extract spatio-temporal dynamics of the data. Likewise, Mehrkanoun et al. [19] proposed a model for predicting temperature and wind speed 1 to 10 days in advance using a convolutional neural network. They introduced an architecture based on 1D-CNNs to process tensor 3D data and to extract spatio-temporal relations. In addition, Hewage et al. [5] presented a weather forecasting model that uses an LSTM and a temporal convolution network. The results obtained are better than classical time series forecasting and classical machine learning. However, these models do not capture the complexities of our specific problem. For instance, we need to deal with multivariate time series forecasting of several time series at different locations. In the aforementioned approaches there are no spatial relations between the entities (e.g. different cities), the interaction is determined by the entity order in the tensor. To capture the spatio-temporal dynamics of different entities, a promising approach is to use Graph Neural Networks, which have the capacity to model temporal dynamics of nodes and spatial dynamics between them at the same time.

Graph neural networks (GNN) have shown recent progress in the area of time series forecasting and spatio-temporal relations. Moreover, a GNN has the ability to extract greater insights compared to networks that can only analyse data in isolation. This is achieved by obtaining structural relationships between the data [20]. There are a number of domains in which GNNs have been successfully applied in recent years, such as traffic flow forecasting, fraud detection, epidemiology and forecasting weather-related events. In regards to the latter, Wilson et al. [21] addressed the spatio-temporal correlation in the data by proposing a deep learning model based on a weighted graph convolutional LSTM. The general goal was to capture temporal autocorrelation with the LSTM and the spatial relationships with the graph convolution. Similarly, Khodayar et al. [22] presented a spatio-temporal Graph convolutional network (GCN) for short-term wind speed forecasting. Another example is the study by Wang et al. [23] which proposed a graph-based model to predict PM2.5 particle concentration and capture the spatio-temporal dependencies.

The most recent advances in GNN have been applied to other domains. For instance, a study by Cheng et al. [7] presented a model using GNN for fraud detection in credit card transactions. They implemented a spatio-temporal attention mechanism which produces the input for a 3D convolution network. As per the previous study, Gao et al. [24] proposed a GNN with spatio-temporal attention mechanism and a GRU architecture to forecast the number of infected cases in a pandemic by considering local disease status, demographic and transmission dynamics. There have been several GNN models applied to traffic flow forecasting and urban planning. In particular, Song et al. [25] developed a spatio-temporal GCN with a synchronous temporal mechanism to predict the flow of a network. Likewise, the studies by Lu et al. [26], Kong et al. [27] and Li et al. [28] proposed different model versions of a spatio-temporal GNN with attention mechanisms for urban sensor value forecasting, traffic flow forecasting and segment-level traffic prediction respectively.

The goal of this study is to predict frost events by using air temperature and humidity data obtained from an IoT system installed on an experimental field and weather stations located around the field. We have two main sources of inspiration. Firstly, we are inspired by recent advancements in GNN models as detailed previously, especially the spatio-temporal attention mechanism. Secondly, we are inspired by the study of Wu et al. [9]





(a) Map of the weather stations and experimen- (b) Schematic version of a graph con-  
tal site. structed at a single time step.

**Figure 1.** Graph modeling based on location of the experimental site and weather stations.

which is a model for multivariate time series forecasting using a GNN and by the recent study of Shang et al. [8] who proposed a model for multivariate time series forecasting using a GNN in which they consider pairwise interactions between features in a node representation. Therefore, the contribution of this paper is a multivariate frost forecasting model based on a GNN with a spatio-temporal attention mechanism.

### 3. Proposal

In this paper, we propose a bivariate time series forecasting model in order to predict the occurrence of frost. The benefit of such a model is that it can be trained with historical time series data  $X = \{x_{t_1}, x_{t_2}, \dots, x_{t_m}\}$  with  $x_t \in \mathbb{R}^2$  the value of the bivariate variable at time  $t$  is used to forecast future values of the variable in a certain time-window  $r$ ,  $Y = \{x_{t_{m+1}}, x_{t_{m+2}}, \dots, x_{t_{m+r}}\}$ . Then, the goal is to create a mapping function from  $X$  to  $Y$  and minimize the loss, typically using a  $l_2$  regularization [9].

In particular, given a set of input data  $P = \{n, temp, hum\}$  and a derived label  $F = \{1, 0\}$  which indicates the presence (1) or absence (0) of frost for each one of the records. We aim to forecast the minimum temperature and the frost class for future time windows  $\{t_m \dots t_{m+r}\}$  based on the historical time window  $\{t_1 \dots t_{m-1}\}$ .

In addition to bivariate time series forecasting, we model the spatial and temporal relationships of weather data from multiple locations. For that purpose we utilize Graph Neural Networks to describe and formalize those relationships. The following are important definitions for graph modeling [9].

- *Graph.* A graph is represented as  $G = (V, E)$  where  $V$  represents the set of nodes and  $E$  represents the set of edges. There are  $n$  number of nodes in a graph.
- *Node Neighborhood.* Describes a set of nodes connected by an edge. A singular node  $v \in V$  and an edge  $e = (v, u) \in E$  maps from  $v$  to  $u$  describes the connection between nodes. The neighborhood of  $v$  is defined as  $N(v) = \{u \in V \mid (v, u) \in E\}$ .
- *Adjacency Matrix.* States the connections between nodes in a graph. It is denoted by a matrix  $A \in \mathbb{R}^{n \times n}$  with  $A_{ij} = q > 0$  if  $(v_i, v_j) \in E$  and  $A_{ij} = 0$  if  $(v_i, v_j) \notin E$ .

Then the graph network is formally defined as  $G = (V, E, A)$  which represents the relationships between nodes in the spatial dimension.

#### 3.1. Data sources

The model was trained and tested using data collected from our IoT platform and 10 meteorological stations, which are all located in the central region of Chile.

The 10 meteorological stations, which are within close proximity of the orchard, provide structured temperature and humidity data in the form of a graph. Here the data is collected every hour. The 10 meteorological stations considered for this study and their representation as a graph are shown in Figure 1.



**Figure 2.** IoT platform installed on the experimental field composed by temperature and humidity sensors.

The IoT platform was developed with both air temperature and air humidity sensors and consists of 12 low-power wireless sensor nodes (motus). The latter are divided into 8 sensor data nodes and 4 repeaters, which are connected to a gateway through a SmartMesh IP manager. The wireless sensor network is exposed directly to environmental conditions (sun, dust, rain, and snow), therefore all sensors are protected by an Internal Protection 65 (IP65) rating enclosure. The IoT platform was installed in a local orchard where data was collected every 10 seconds at four different heights above ground (one, two, three and four meters). An image of the IoT platform in situ in the orchard is shown in figure 2.

Data was collected between the 4th of September, 2020 until the 5th of April, 2021. Training data was taken from the months of September to February and the last two months of data were used for training. It is assumed that environmental factors can have an accumulated impact on frost, therefore the prediction is done using time series data. For this reason, we need the model to learn time-related patterns, which is why we do not randomly split training and testing data.

All the data is preprocessed for missing values and outliers. Data from the IoT platform is downsampled using 1 minute time-windows. In addition, to map the frequency of both data sources, data from weather stations is linearly interpolated. Finally, in case of the classification of frost, a label is created in the training data with two classes (Frost / No Frost) and given the imbalance between them, the SMOTE method was applied.

### 3.2. Forecasting model

In this study, we develop a GRAFT-Frost model, the architecture of which is shown in Figure 3. Firstly, we convert our input  $P$  into a three-dimensional (spatial, temporal and features) high order tensor representation  $\mathcal{X}$ . The tensor is then fed into the graph neural network, which aims to correlate the IoT platform data with that of the meteorological stations. For each  $t$  we create a graph of nodes that relate to each of the stations (meteorological and the IoT platform) and their corresponding edges. Then, we apply a spatio-temporal attention mechanism and a 3D convolution layer to obtain a feature-learned tensor  $\mathcal{X}^c$ . With spatio-temporal attention and 3D convolution, the idea is to weigh the importance of different dimensions and find hidden patterns from the input data. Finally,  $\mathcal{X}^c$  is fed through a recurrent neural network to produce a forecast with two different loss functions depending on the type of task. We present details of each part of this architecture in the following subsections.

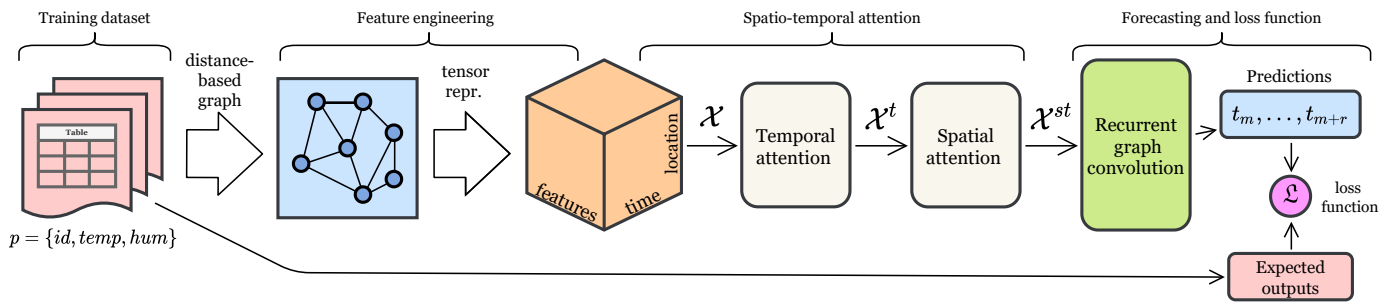


**Figure 3.** Overview of the GRAST-Frost model.

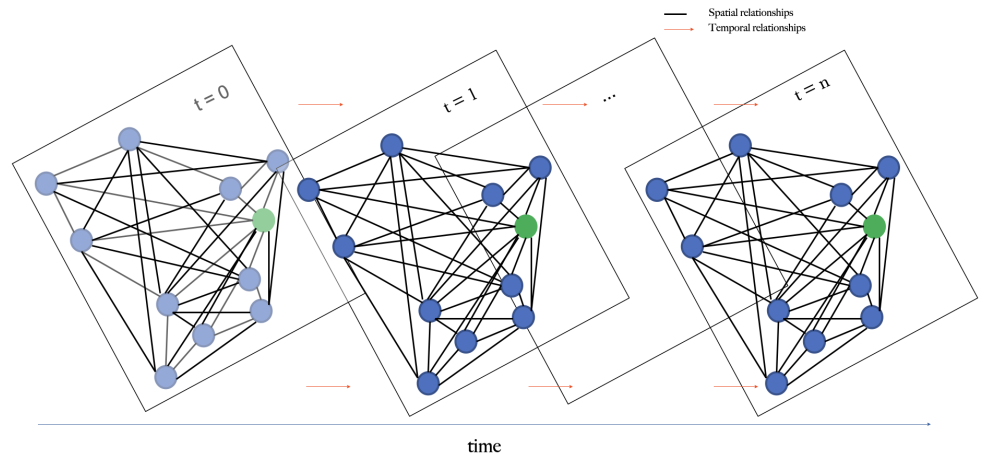


**Figure 4.** Schematic view of the spatio-temporal graph network for modeling the relationships between the experimental field and weather stations through time.

1 In order to forecast local weather conditions at the orchard using the aforementioned  
 2 sensory data, we predict at differing time intervals into the future (6, 12, 24 and 48 hours).  
 3 At a single time step the geographical locations of the nodes are graphed as can be seen in  
 4 Figure 1, where the blue dots represent the meteorological sites and the green dot depicts  
 5 the experimental site. For multiple time steps, the graph is expanded into a spatio-temporal  
 6 graph where feature values for a given node are related to its previous and future values,  
 7 and its spatial neighbors. A schematic view of this idea is shown in Figure 4.

### 8 3.2.1. Feature Engineering

9 In order to represent the input data as a tensor  $\mathcal{X} \in \mathbb{R}^{T \times S \times F}$  where  $T$ ,  $S$ , and  $F$  denote  
 10 the temporal, spatial and feature dimensions. In particular, for each spatio-temporal pair  
 11 composed of a certain time horizon and location, a feature vector is built ( $f \in \mathbb{R}^F$ ) based  
 12 on the measurements collected in that pair. There are a total of  $T \times S$  spatio-temporal pairs,  
 13 each one of them are features of  $F$  dimensions. Based on [7], the feature vector is composed  
 14 of two parts: feature measurements and graph features. For measurements we include raw  
 15 temperature, humidity data, mean, standard deviation, median, maximum and minimum  
 16 values for a specific time horizon. For the graph related features, we include several metrics  
 17 obtained from the graph neural network processing described in the following section.

### 18 3.2.2. Graph construction at a single time step

19 Given the tensor  $X$ , the geographical location (latitude, longitude) of the weather  
 20 stations and experimental field is obtained. This data is used to calculate the geographical  
 21 proximity which in turn contributes to the development of the adjacency matrix. Nodes  
 22 are simply a subset of the tensor in time  $t$ . We utilize an aggregation function to reduce



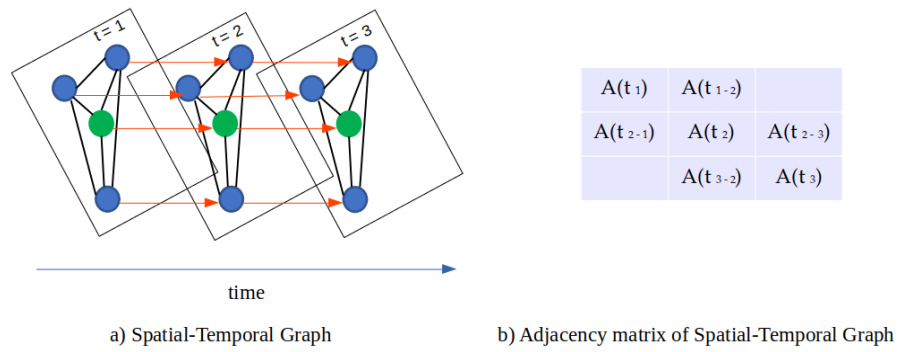


**Figure 5.** Spatio-temporal graph construction and adjacency matrix for including multiple time steps.

23 the edge updates to a single element. Therefore, for a single node, we summarize the  
24 interactions with other nodes.

25 *Graph nodes.* The nodes in the graph  $G(V, E)$  are constructed to represent input  
26 data, by associating features such as  $(temp, hum)$  and location  $(lat, lon)$ . In total we have  
27 11 nodes. Generally, we have two types of nodes: Be  $v$  the node corresponding to the  
28 experimental field and  $u$  the node corresponding to the weather stations. Thus,  $f_v$  and  $f_u$   
29 are the correspondent feature vectors for each one of them.

*Graph edges.* The edges are constructed based on geographical distance between nodes.  
We construct a weighted graph where the weight is inversely proportional to distance.  
Formally, in a weighted graph  $G = (V, E, w)$  [6], that do not contain any cycle of negative  
weight, the distance between node  $u$  and  $v$  is defined as  $d : V \times V \rightarrow \mathbb{R}$  as

$$d(u, v) = \begin{cases} 0 & \text{if } u = v, \text{ and} \\ \|(location_u, location_v)\| & \text{otherwise.} \end{cases} \quad (1)$$

30 which is the Euclidean distance between the location of nodes  $u$  and  $v$ .

Therefore, the weight is,

$$w_{uv} = \frac{1}{d(u, v)} \quad (2)$$

31 For this study, all nodes are integrated, thus, there are edges between all of the  
32 nodes. Therefore, the feature vector of the edge is  $f_e = w_{uv} * f_{gmn}$ , which is the weighted  
33 measurement of  $f_{gmn}$ , features to be obtained by the graph neural network (GNN).

### 34 3.2.3. Spatial-temporal graph construction

35 In order to represent the relationship between each node and its neighbors across time,  
36 inspired by [25], we connect all nodes with themselves sequentially for each time step.  
37 This allows us to create a spatial-temporal graph by sequentially connecting nodes from  
38 previous, to current and future time steps as shown in figure 5. Therefore, it is possible to  
39 understand the relationships between nodes through time. In practice, we create a new  
40 adjacency matrix  $A^T \in \mathbb{R}^{n \times T}$  for the spatial-temporal graph. The new adjacency matrix  
41 can be formulated simply as

$$A_{i,j}^T = \begin{cases} 1 & \text{if } v_i \text{ is related with } v_j, \\ 0 & \text{otherwise.} \end{cases} \quad (3)$$

42 As illustrated in Figure 5 the new adjacency matrix has dimension  $N \times T$  where its  
43 diagonal represents the adjacency matrix for a single time step and a relation of the nodes  
44 through time.

45 For each time step a GNN consumes the graph described on the previous section. The  
46 information of interactions between nodes is described in terms of nodes involved  $u, v$ ,  
47 time  $t$ , location  $l$  and measurement  $m$ . Based on it, the edges are constructed. Features for

48 nodes  $f_v, f_u$  and edges  $f_e$  are initialized accordingly. Then, we iteratively include graph  
 49 constructed in subsequent time steps by updating the representation of nodes and edges  
 50 based on the previous time step and weighted by the adjacency matrix  $A^T$ . Edges features  
 51 are updated as follows:

$$f_{euv}^t = FC_e(f_{euv}^{t-1}, id_u, id_v, A_{t,t-1}^T) \quad (4)$$

52 Where  $f_{euv}^t$  is the edge feature between nodes  $u$  and  $v$  in the time  $t$ ,  $FC_e$  is a fully  
 53 connected neural network with a *ReLU* activation function which computes all the edges  
 54 updates. In addition,  $id_u, id_v$  are the location on graph of node  $u$  and  $v$ . Then, for each time  
 55 step we proceed to update the node features  $f_u$  and  $f_v$ . For each node we sum all the edges  
 56 that are connected to that node. Regarding  $f_v$  the equation is the following:

$$f_v^t = FC_v\left(\sum_i^N f_{e_i}^t, f_v^{t-1}, A_{t,t-1}^T\right) \quad (5)$$

57 Here  $f_v^t$  is the node feature in time  $t$ ,  $N$  is the total number of nodes and  $FC_v$  is a fully  
 58 connected neural network.

59 Finally, we calculate the feature vector of the graph  $f_g$  which is the average of all the  
 60 updates of  $f_e$  and  $f_v$  for every time step.

61 The output of the GNN are the updated values of  $f_v, f_u, f_e$  and  $f_g$ . We use these values  
 62 to complete the feature vector  $F$  on the tensor  $\mathcal{X}$  regarding the graph part, as described in  
 63 the previous section.

#### 64 3.2.4. Spatio-temporal attention mechanism

65 The idea of the attention network is to weigh the importance of spatial and temporal  
 66 values from the current measurement for a specific node and time. We use the GAT model  
 67 [6] to extract Spatio-temporal similarity features. The idea is to update the embedding  
 68 information of each node using the aggregate data from its neighbors. Therefore, weather  
 69 stations and the IoT platform receive prior temperature and humidity data from nearby  
 70 areas. This allows us to hypothesize that a specific prediction is more likely due to a higher  
 71 importance being given to meteorological sites in close proximity to the orchard, rather  
 72 than those located further away, and recent measurements being given a higher priority  
 73 compared to older measurements. It should be noted that given the feature tensor  $\mathcal{X}$  we  
 74 can query the temporal values  $\forall t \mathcal{X}_{tsf}$  ( $t \in \{1, 2, \dots, T\}$ ) to extract the time horizon, and the  
 75 spatial values  $\forall s \mathcal{X}_{tsf}$  ( $s \in \{1, 2, \dots, S\}$ ) to extract the location coordinates.

#### 76 Temporal attention

77 In the temporal dimension, there exists correlations between temperature and humid-  
 78 ity values in different time steps. Since weather is highly dynamic, temporal correlations  
 79 are variable under different conditions. Therefore, in order to have a mechanism for cap-  
 80 turing those correlations, we use attention to adaptively obtain the importance of past data  
 81 in relation to current data.

82 Based on [7], considering a tensor  $\mathcal{X}$ , the temporal attention layer is the temperature  
 83 and humidity values for a specific time multiplied by a weighted sum of the matrix  
 84 representation of all temporal values. Formally, it is described as

$$\mathcal{X}^t = \sum_{t=1}^T a_t \mathcal{X}_{tsf} \text{ with} \quad (6)$$

$$a_t = \frac{\exp((1 - \lambda_t) \cdot FC_t(W_t, \mathcal{X}_{tsf}))}{\sum_{t=1}^T \exp((1 - \lambda_t) \cdot FC_t(W_t, \mathcal{X}_{tsf}))}. \quad (7)$$

85 Here  $a_t$  is the weight for each time step,  $FC_t$  is a fully connected layer with *ReLU*  
 86 activation and the weight vector  $W_t$ ;  $\lambda_t \in [0, 1]$  is the temporal penalty factor to control the

87 importance of temporal attention;  $\mathcal{X}^t$ , the output of the temporal attention layer is a tensor  
88 with  $\mathcal{X} \in \mathbb{R}^{T \times S \times F}$ .

### 89 Spatial attention

90 Considering the spatial dimension, temperature and humidity values from different  
91 nodes have varying influences and due to weather behavior these influences are highly  
92 dynamic. In particular, we are interested in capturing correlations between the nodes on  
93 the weather values in the spatial dimension. Therefore, we want to explicitly capture the  
94 relationships between close and distant nodes.

95 Given the output from the temporal attention layer  $\mathcal{X}^t$ , the spatial attention mecha-  
96 nism is applied. Formally it is described as

$$\mathcal{X}^{st} = \sum_{s=1}^S a_s \mathcal{X}_{tsf}^t \text{ with} \quad (8)$$

$$a_s = \frac{\exp((1 - \lambda_s) \cdot FC_s(W_s, \mathcal{X}_{tsf}^t))}{\sum_{s=1}^S \exp((1 - \lambda_s) \cdot FC_s(W_s, \mathcal{X}_{tsf}^t))}. \quad (9)$$

97 Where  $W_s$  is the weight of the fully connected spatial network  $FC_s$ ; and  $\mathcal{X}^{st}$  is the  
98 output of both self-attention layers. The output is reshaped into a tensor format with the  
99 same order as  $\mathcal{X}$ ;  $a_s$  is the weight for each spatial step;  $\lambda_s \in [0, 1]$  is the spatial penalty  
100 factor to control the importance of spatial attention.

### 101 3.2.5. Convolution process

102 Several studies have stated the benefits of applying convolutional neural networks  
103 to feature tensors based on graph neural network modeling [29–31]. In our case we use a  
104 3D Convolutional Network with the  $\mathcal{X}^{st}$  tensor as an input. The idea is to extract hidden  
105 patterns from spatio-temporal features by stacking multiple layers in the architecture.

The 3D convolution is represented as

$$\mathcal{X}_k^c = \sum_k \mathcal{X}^{c-1}(d_t - c_a, d_s - c_b, d_f - c_q) \mathcal{K}_i^l(c_a, c_b, c_q). \quad (10)$$

106 Here  $\mathcal{K}_i^l$  is a 3D kernel in the  $l^{th}$  layer and  $i^{th}$  kernel in a convolution with feature  $\mathcal{X}^{c-1}$ .  
107 In particular the 3D convolution kernel is  $(c_a, c_b, c_q)$ . It should be noted that the first layer  
108 of  $\mathcal{X}^{c-1}$  is the output of our attention mechanism  $\mathcal{X}^{st}$ .  $d_t, d_s$ , and  $d_f$  are the dimensions of  
109  $\mathcal{X}^{st}$  considering temporal, spatial and feature components, which equals to  $T, S, F$  of the  
110 first convolution layer.

Finally, the output feature  $\mathcal{X}^c$  is

$$\mathcal{X}^c = \sigma\left(\sum_k \mathcal{X}_k^c + b^c\right), \quad (11)$$

111 where  $b^c$  is the bias parameter and  $\sigma$  is the sigmoid function.

### 112 3.2.6. Graph neural network forecasting

113 In the last part of the forecasting model, we apply a Recurrent Neural Network to  
114 capture the sequential aspect of the problem and produce forecasts based on historical  
115 data. Given the tensor  $\mathcal{X}^c$  we use a sequence-to-sequence model (seq2seq) [32] over each  
116 node, ie  $\forall s \mathcal{X}_{tsf}^c$ . Thus, we extract the transformed series from the experimental field and  
117 weather stations. The reason for using seq2seq is that in a graph structure, we can perform  
118 recurrent graph convolution to handle all series simultaneously [8]. In practice, for each  
119 series we used  $\{t_1, \dots, t_{m-1}\}$  time values to train the model and  $\{t_m, \dots, t_r\}$  to forecast the  
120 weather using  $r \in \{6, 12, 24, 48\}$  hours in the future. Specifically, for each time  $t$ , the seq2seq  
121 model takes  $\mathcal{X}_{tsf}^c \forall s$  for all series and updates the internal hidden state from  $H_{t-1}$  to  $H_t$ .  
122 The encoder recurrently updates the training data to be included, producing  $H_{t+r}$  as a

123 summary. The decoder takes that input and continues the recurrence to include all the  
124 testing data for the forecasting phase.

Finally, we use two loss functions, one for classification and one for regression. The former loss function is defined as

$$\mathcal{L} = \frac{-1}{N} \sum_{i=1}^N [y_i \log(H_i) + \beta(1 - y_i) \log(1 - H_i)], \quad (12)$$

125 where  $N$  is the total number of samples in the series,  $\beta$  is a sample weight regarding the  
126 distribution of Frost/No Frost;  $y_i \in \{0, 1\}$  is the real label and  $H_i$  is the value score produce  
127 by the forecasting.

The regression loss function uses mean squared error

$$\mathcal{L} = \frac{1}{N} \sum_{i=1}^N |y_i - H_i|^2. \quad (13)$$

## 128 4. Results

### 129 4.1. Baselines and evaluation metrics

130 We use our model to solve a regression problem, to predict the minimum temperature  
131 in all the nodes, and a classification problem, to predict two classes Frost and No Frost. In  
132 case of regression, we compare with the following forecasting methods:

- 133 1. Non-deep learning methods: historical average (HA), ARIMA with Kalman filter  
134 (ARIMA), vector auto-regression (VAR), and support vector regression (SVR). The  
135 historical average accounts for weekly seasonality and predicts for a day by using the  
136 weighted average of the same day in the past few weeks.
- 137 2. Deep learning methods that produce forecasting for each series separately (no graph-  
138 based) such as feed-forward neural network (FNN) and LSTM.
- 139 3. Autoencoder forecasting method with attention mechanism (AC-att).
- 140 4. Graph convolutional network applied on the given graph without spatio-temporal  
141 attention mechanism (GCN).
- 142 5. Variants of this architecture using convolutions [7] and GRU [24].

143 In case of classification, we do not use the non-deep learning methods described  
144 above, but we use support vector machines (SVM) and tree-based classification algorithms  
145 such as naïve Bayes and XGBoost.

146 For regression, all methods are evaluated with three metrics: mean absolute error  
147 (MAE), root mean square error (RMSE), and mean absolute percentage error (MAPE). For  
148 classification, all methods are evaluated with Precision, Recall and F1 metrics.

### 149 4.2. Hyperparameters

150 Several hyperparameters are tuned through grid search: initial learning rate in  
151  $\{0.1, 0.01, 0.001\}$ , dropout rate in  $\{0.1, 0.2, 0.3\}$ , embedding size of the LSTM layer was  
152 set in  $\{32, 64, 128, 256\}$ , the  $k$  value in kNN in  $\{5, 10, 20, 30\}$ , and the weight of regulariza-  
153 tion in  $\{0, 1, 2, 5, 10, 20\}$ . For other hyperparameters, the convolution kernel size in the  
154 feature extractor is 10 and the decay ratio of learning rate is 0.1. After tuning, the best  
155 initial learning rate for our dataset is 0.001. The optimizer is Adam.

156 All models are implemented in PyTorch and ran in the Google Colaboratory platform.

### 157 4.3. Results for regression problem

158 Table 1 and Figure 6 show the evaluation of the proposed GSTA-RCN model compared  
159 with the baselines. The tasks are to forecast the minimum temperature of the experimental  
160 field with 6 h, 12 h, 24 h and 48 h in advance.

161 The proposed model outperforms all the compared baselines for frost forecast in 6 h,  
162 12 h, 24 h and 48 h tasks. It is noticeable that a non-graph model such as an autoencoder  
163 with an attention mechanism outperforms GNN with spatio-temporal attention using

Table 1: Average MAE, RMSE and MAPE metrics of time series forecasting models applied to frost forecast.

Model	MAE			RMSE			MAPE		
	6 h	12 h	24 h	6 h	12 h	24 h	6 h	12 h	24 h
VAR	5.79	5.80	6.82	8.81	9.78	12.79	8.74	9.64	12.23
FNN	4.28	4.76	5.74	7.88	8.60	10.75	7.21	8.77	9.98
LSTM	4.03	4.76	5.46	6.93	7.35	9.11	6.95	6.89	8.61
AC-att	3.41	3.79	4.26	5.89	6.64	7.44	5.74	5.84	7.05
GCN	3.61	3.89	4.28	6.01	7.09	7.46	5.55	5.89	7.03
STA-C	3.77	4.02	4.83	6.55	8.02	8.71	6.11	7.87	8.30
STA-GRU	3.52	3.73	4.17	6.14	7.20	7.39	5.82	5.99	7.05
<b>GRAST-Frost</b>	<b>3.08</b>	<b>3.25</b>	<b>3.86</b>	<b>5.42</b>	<b>5.79</b>	<b>6.19</b>	<b>5.39</b>	<b>5.44</b>	<b>6.04</b>

convolution and GRU. To improve these results it is necessary to collect more weather data, more weather variables and use more weather stations for modeling geographical and temporal interactions.

In general terms, we can separate the results from non-deep learning models and FNN from LSTM, autoencoder and graph-based neural network architectures. Non-deep learning models (HA, ARIMA) and the simple deep learning architecture FNN only have similar error scores with the other architectures on the 6 h task. For a greater time-window their performance drastically decreases. Then, we can compare results from LSTM with the results from STA-C, the variation of the spatio-temporal GNN with attention mechanism and a convolution-based forecasting method. For this dataset, the complexity added by STA-C does not have an impact in the performance of the model and a simple LSTM is preferable, especially for 6 h, 12 h and 24 h predictions. As mentioned previously, the autoencoder architecture with attention mechanism performs better than STA-C and similar to STA-GRU for 6 h, 12 h and 24 h tasks. Finally, our model outperforms all the previous baselines. In our case the complexity of the modeling successfully increases the performance of the prediction for each time-window task.

Figure 7 shows models results in terms of RMSE for the experimental field node and the three geographically closest node neighbors. By focusing on the prediction for each node, instead of the average of all nodes, the results description remains the same. In addition, the Pearson correlation statistic is calculated to compare model prediction with time windows. The performance of all models decreases when the time-window increases, and its results are variable in the different nodes. Therefore, the behavior of models regarding time-window is different in each node, which is a result that could be worth to continue studying.

In addition, Figures 9 and 8 show real and predicted data for a specific day. In Figure 8 we present the variation of our model prediction regarding 6 h, 12 h, 24 h, and 48 h tasks. It is clearly shown that our model best performance is in the 6 h window task and then the performance decreases gradually. It can be noted that although the performance decreases for larger time windows, our model is capable of detecting the temperature trend. The range of the error interval increases if we want to make the prediction point by point, but if that range is detected, we can be sure that the prediction is reliable. Figure 9 shows our model prediction and the second-best prediction (STA-GRU) in the 6 h task. Both models detect the temperature trend, but in our model the error range is smaller.

#### 4.4. Results for classification problem

Table 2 and Figure 10 show the evaluation of the proposed GSTA-RCN model compared with the baselines as a classification problem. In this problem, two classes are predicted: Frost (temperature below 0 °C) and No Frost (temperature above 0 °C).



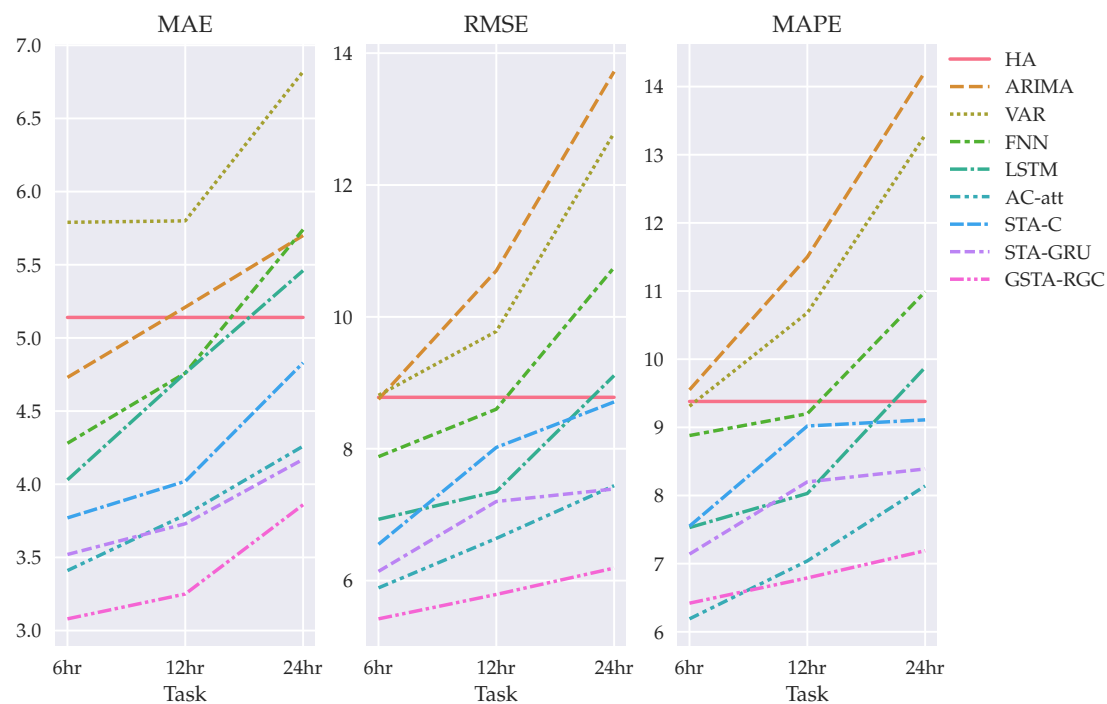


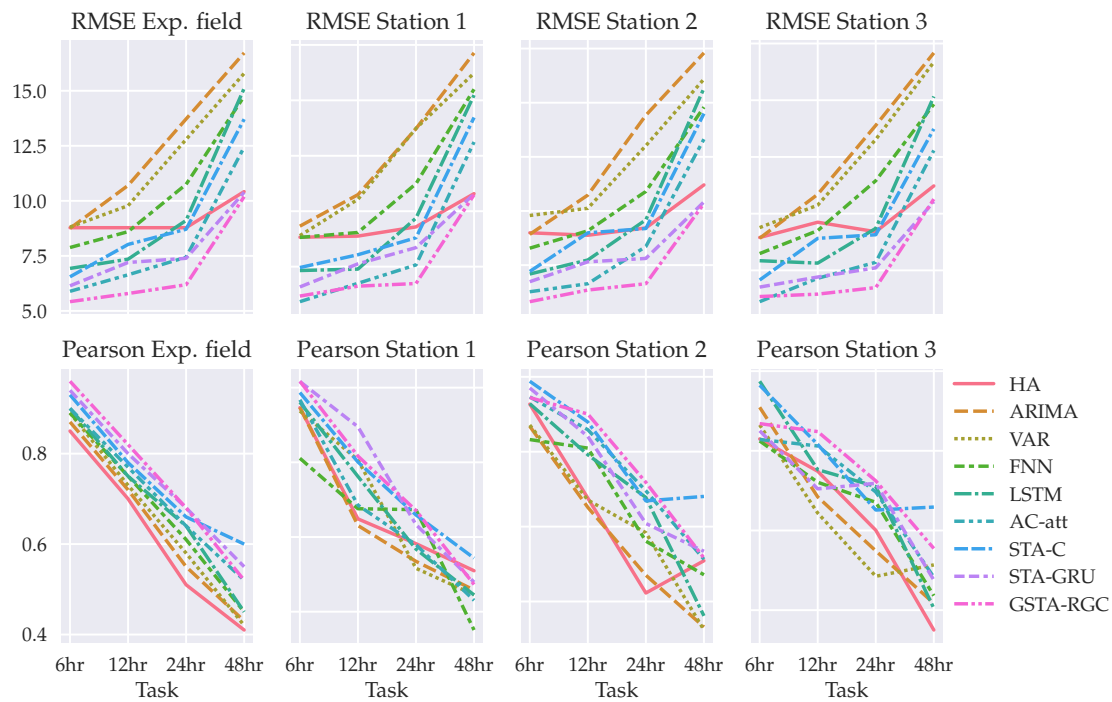
Figure 6. MAE, MAPE and RSME metrics results for temperature forecasting on 6, 12 and 24 hours in advance.

Table 2: Average Precision, recall and F1 metrics for classification of frost events according different models implementations.

Model	Precision			Recall			F1		
	6 h	12 h	24 h	6 h	12 h	24 h	6 h	12 h	24 h
SVM	0.569	0.535	0.513	0.565	0.529	0.507	0.555	0.531	0.502
XGBoost	0.754	0.740	0.713	0.749	0.730	0.701	0.748	0.716	0.711
FNN	0.644	0.643	0.638	0.663	0.658	0.639	0.690	0.669	0.658
LSTM	0.675	0.666	0.652	0.695	0.650	0.632	0.682	0.647	0.641
AC-att	0.713	0.709	0.690	0.705	0.700	0.696	0.699	0.691	0.671
GCN	0.792	0.787	0.780	0.784	0.778	0.769	0.806	0.802	0.787
STA-C	0.814	0.797	0.794	0.837	0.810	0.809	0.830	0.826	0.784
STA-GRU	0.845	0.844	0.824	0.850	0.821	0.805	0.863	0.845	0.842
<b>GRAST-Frost</b>	<b>0.891</b>	<b>0.876</b>	<b>0.848</b>	<b>0.898</b>	<b>0.882</b>	<b>0.845</b>	<b>0.908</b>	<b>0.869</b>	<b>0.863</b>

201 In this case our model also outperforms all the baselines for the 6 h, 12 h, 24 h, and 48 h  
 202 tasks. In addition, similar to regression, models performance decreases when time-window  
 203 increases.

204 For this dataset, naive Bayes and SVM models provides the worst predictions, espe-  
 205 cially for recall score which implies a high value of false negative predictions. Comparing  
 206 with regression, in classification FNN and LSTM perform similar. It is worth to remark  
 207 that the autoencoder with attention mechanism is slightly better that the previous ones but  
 208 performs worse than all the graph-based models and even the XGBoost model. Figure 10  
 209 shows that for classification in this dataset the graph-based models are preferable. In this  
 210 case the spatio-temporal attention mechanism in the GNN which captures the dynamics  
 211 between the nodes is a key factor to improve the predictions. In particular, in our model  
 212 the strategy to use the spatio-temporal vectors to perform the prediction at the same time  
 213 obtains the best results by minimizing classification errors which can be valuable for real  
 214 world applications.



**Figure 7.** RMSE and Pearson statistic results regarding forecasting on the experimental field and the three nearest weather stations.

**Table 3:** T-test for comparing our regression model with baselines for 6 h, 12 h, 24 h and 48 h forecasts.

Model	6 hours		12 hours		24 hours		48 hrs	
	$t$	$p$ -value	$t$	$p$ -value	$t$	$p$ -value	$t$	$p$ -value
HA	9.662	0.011	7.716	0.022	7.398	0.028	7.276	0.031
ARIMA	9.673	0.012	9.443	0.026	8.534	0.0036	8.139	0.033
VAR	10.330	0.017	8.247	0.041	7.831	0.045	7.172	0.044
FNN	5.946	0.020	5.722	0.025	5.595	0.030	4.239	0.041
LSTM	6.540	0.029	6.260	0.024	5.144	0.039	4.136	0.045
AC – att	4.293	0.017	3.674	0.020	3.562	0.025	3.179	0.035
STA – C	3.314	0.011	2.980	0.014	2.593	0.019	2.284	0.041
STA – GRU	1.387	0.030	1.271	0.038	1.009	0.041	0.766	0.081

## 215 5. Discussion

### 216 5.1. GNN and spatio-temporal attention applied to frost forecast

217 The first research question pretends to evaluate the performance of the graph neural  
 218 network against current state-of-the-art models for frost forecasting. In other words, does  
 219 the use of a deep learning model with graph-based data improves the performance of a  
 220 predictor?

221 The overall results indicate that our model outperforms previous frost forecasting  
 222 models and most of the variations presented for graph neural networks. To statistically  
 223 check whether the models' performance difference is significant, we conducted a t-test  
 224 between our model and each previously proposed frost forecasting model and other base-  
 225 lines presented. Tables 3 and 4 shows the statistics results for regression and classification  
 226 respectively.

227 As can be seen in Tables 3 and 4 there is statistical significance for the results of our  
 228 model against all previously proposed frost forecasting models for 6 h, 12 h, 24 h and 48 h  
 229 in advance predictions. More generally, for all the baselines presented, there are some  
 230 exceptions in the 48 h time-window prediction since there is no evidence of a difference

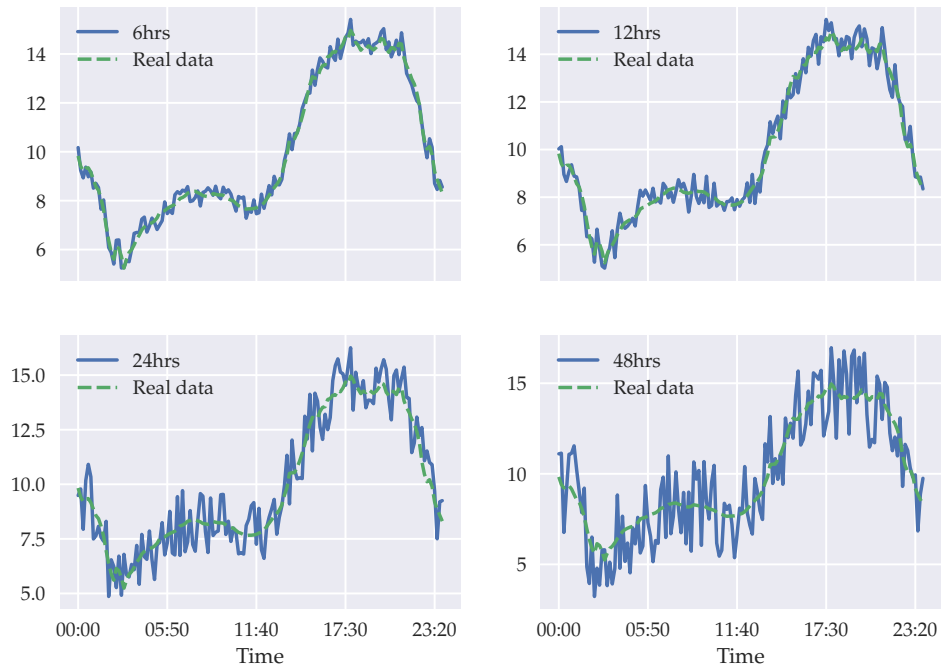


**Figure 8.** GRAST-Frost model results compared with real data for 6, 12, 24 and 48 hours forecasts.

**Table 4:** T-test for comparing our classification model with baselines for 6 h, 12 h, 24 h and 48 h forecasts.

Model	6 hours		12 hours		24 hours		48 hrs	
	$t$	$p$ -value	$t$	$p$ -value	$t$	$p$ -value	$t$	$p$ -value
<i>SVM</i>	9.610	0.015	9.042	0.036	7.946	0.038	7.939	0.049
<i>NB</i>	9.527	0.023	8.129	0.032	7.139	0.045	7.051	0.046
<i>XGBoost</i>	3.786	0.013	3.712	0.022	3.467	0.041	3.378	0.043
<i>FNN</i>	6.765	0.016	6.002	0.026	4.758	0.030	4.206	0.036
<i>LSTM</i>	6.095	0.018	5.245	0.018	4.586	0.026	4.488	0.046
<i>AC – att</i>	4.886	0.025	4.398	0.029	3.665	0.034	3.479	0.040
<i>STA – C</i>	3.018	0.023	2.579	0.029	2.152	0.047	2.084	0.048
<i>STA – GRU</i>	1.476	0.039	1.094	0.036	0.986	0.047	0.713	0.071

231 between our model and STA-GRU. This result can be used for future research with the  
 232 purpose of improving the performance in larger-time windows.

233 The second research question “Does the spatio-temporal attention mechanism im-  
 234 proves the forecast?” is approached similarly to the previous one. In this case, we are  
 235 interested to statistically check whether there is a difference between the performance  
 236 of our model with GNN models that do not use spatio-temporal attention mechanisms.  
 237 In particular, table 5 shows the results of a t-test applied between our model,  $GCN_{reg}$   
 238 and  $GCN2_{clas}$  separately for regression and classification problems. As a result, we can  
 239 demonstrate that for our dataset, results are statistically different between our model and  
 240 non-spatio-temporal attention graph-based models.

241 The last research question, regarding whether the combined use of different data  
 242 sources improve the forecast, in comparison with using a single data source, can be  
 243 answered based on the first two questions. By answering the two first research questions we  
 244 are implicitly answering the last one since the use of different data sources imply on the  
 245 use of weather data collected from different locations. Therefore, it is possible to construct  
 246 the graph and collect the spatial relationships between the nodes which is crucial for the  
 247 model’s performance.

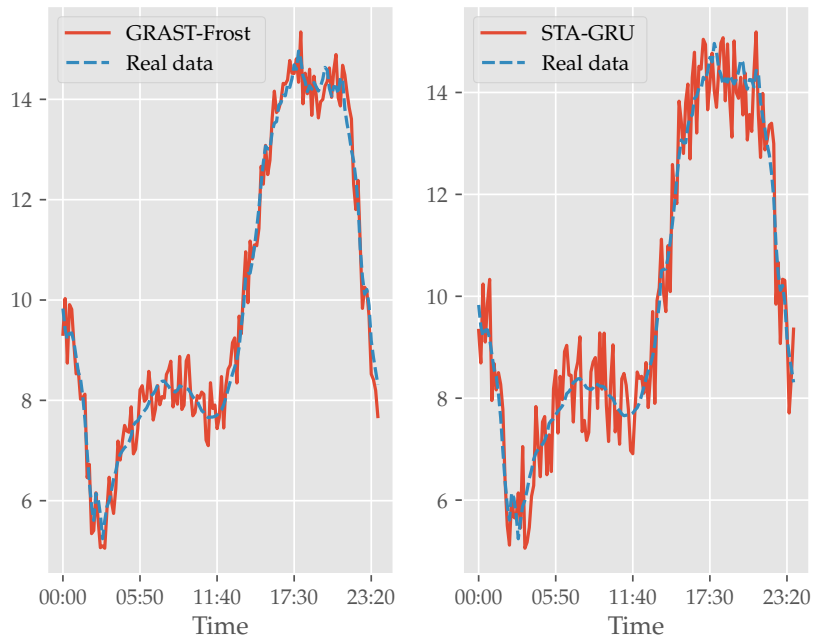


**Figure 9.** On the left there is a comparison of GRAFT-Frost model with real data. On the right there is a comparison of STA-GRU model with real data.

Table 5: T-test for comparing our model with graph-based models without spatio-temporal attention for 6 h, 12 h, 24 h and 48 h forecasts.

Model	6 hours		12 hours		24 hours		48 hrs	
	$t$	$p$ -value	$t$	$p$ -value	$t$	$p$ -value	$t$	$p$ -value
$GCN_{reg}$	3.631	0.013	3.412	0.018	2.456	0.033	2.416	0.035
$GCN_{clas}$	4.009	0.012	3.861	0.031	2.859	0.032	2.787	0.041

248 Finally, in terms of an evaluation for the IoT based system in comparison with the  
 249 weather stations used, as shown in figure 7 the overall results indicate that there is no  
 250 difference between sites. Concretely, Table 6 presents statistics by comparing the prediction  
 251 results of using our model in the experimental field against each weather station. As noticed,  
 252 there is no statistically significance that indicate a performance difference. Therefore, data  
 253 collected from our system is reliable.

## 254 5.2. Limitations

255 The main limitation of this model concerns with the decrease of performance with  
 256 larger time-windows. Despite that it is a problem for all the models studied in this  
 257 paper, the performance difference of our model in short-term windows with all models  
 258 cannot be established in 48 h time-windows. We suspect that this behavior is similar for  
 259 even larger time-windows. The lack of statistical significance, in those specific cases, is  
 260 probably a consequence of a constrained period of time in which we collected the data from  
 261 the experimental site and weather stations. Consequently, model performance should be  
 262 revisited when the amount of data collected is larger, one year and more. However, it is also  
 263 interesting to deeply study the deep learning architecture used and to investigate whether  
 264 further improvements can be made to obtain better results for long-term predictions.

## 265 6. Conclusions

266 We have presented our frost forecasting model that uses and optimizes a graph  
 267 structure between multiple time series using a GNN architecture with a recurrent graph  
 268 convolution mechanism to process each series simultaneously. The model concludes with  
 269 spatio-temporal attention to consider spatial relations and extract temporal dynamics.

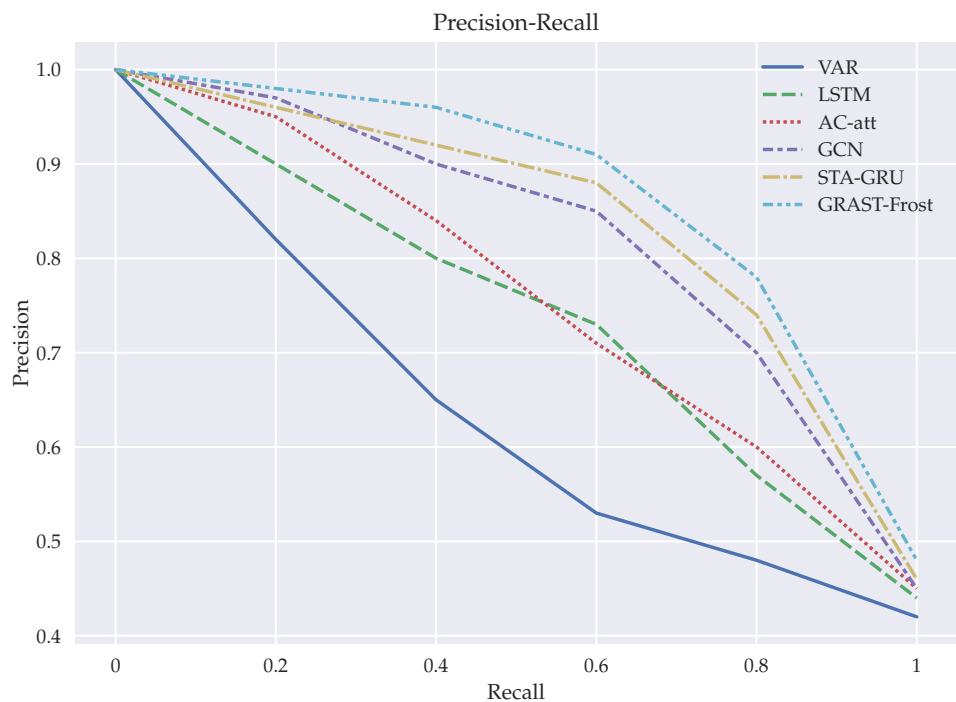


**Figure 10.** ROC curve comparing GRAST-Frost with other models implementations.

Table 6: T-test for comparing our model forecast results from the experimental site with weather stations

Model	6 hours		12 hours		24 hours		48 hrs	
	$t$	$p$ -value	$t$	$p$ -value	$t$	$p$ -value	$t$	$p$ -value
WS1	0.963	0.075	0.810	0.070	0.764	0.098	0.665	0.093
WS2	0.843	0.071	0.683	0.061	0.629	0.069	0.540	0.084
WS3	0.802	0.075	0.676	0.075	0.568	0.081	0.501	0.083
WS4	0.821	0.064	0.731	0.064	0.691	0.078	0.593	0.088
WS5	0.915	0.09	0.025	0.102	3.921	0.136	4.326	0.119
WS6	0.817	0.111	0.660	0.081	0.607	0.105	0.535	0.116
WS7	0.930	0.087	0.703	0.099	0.669	0.092	0.653	0.099
WS8	0.915	0.078	0.025	0.083	3.921	0.118	4.326	0.139
WS9	0.924	0.060	0.918	0.086	0.740	0.111	0.723	0.118
WS10	0.903	0.094	0.794	0.097	0.741	0.126	0.602	0.137

270 Frost forecast is an important area of climate research because of its economic impact  
 271 on several industries. In this study, a GNN with spatio-temporal architecture has been  
 272 proposed to predict minimum temperatures at an experimental site. The model considers  
 273 spatial and temporal relations and processes multiple time series simultaneously. Perform-  
 274 ing predictions of 6, 12, 24 and 48 hours this model outperforms statistical and non-graph  
 275 deep learning models.

276 To further improve this model, we will continue our research by studying deep learn-  
 277 ing architectures to specifically adapt to different time-window forecasts. In addition, we  
 278 aim to include domain knowledge from climate sciences that could help in the construction  
 279 of the graph to transit from a statically-defined to a dynamically-defined graph. Finally,  
 280 by including domain knowledge or by applying new methods, we want to extract the  
 281 influences of the nodes with each other for purposes of explaining the dynamics of the  
 282 graph and, as a consequence to provide better practical insights to users of the system.

283 **Funding:** This research was funded by CORFO/ANID International Centers of Excellence Program  
 284 10CEII-9157 Inria Chile and CORFO "Crea y Valida" Project 19CV-107497.



285 **Institutional Review Board Statement:** Not applicable.

286 **Informed Consent Statement:** Not applicable.

287 **Acknowledgments:** In this section you can acknowledge any support given which is not covered by  
288 the author contribution or funding sections. This may include administrative and technical support,  
289 or donations in kind (e.g., materials used for experiments).

290 **Conflicts of Interest:** The authors declare no conflict of interest.

#### 291 **Appendix A Weather Stations considered on the study**

- 292 1. Campanacura (36°12' 48.0" S,71°44' 15.0" W)
- 293 2. Copihue (36° 04' 32,0" S,71° 45' 29.0" W)
- 294 3. Longavi Norte (36° 02' 13.0" S,71° 40' 60.0" W)
- 295 4. Los Despachos (36° 03' 44.0" S,72° 22' 17.0" W)
- 296 5. Monte-flor Tucapel (36° 14' 41.0" S,71° 56' 03.0" W)
- 297 6. Parral (36° 12' 48,0" S,71° 44' 15.0" W)
- 298 7. Odjfell (36° 08' 24,0" S,72° 16' 12.0" W)
- 299 8. Parral Norte (36° 13' 49.0" S,71° 43' 56.0" W)
- 300 9. Ñiquen (36° 17' 37.0" S,71° 53' 17.0" W)
- 301 10. CE Arroz (36° 24' 33.0" S,72° 00' 24.0" W)

## References

1. M. Á. Guillén-Navarro, F.P.G.; Martínez-España, R. IoT-based System to Forecast Crop Frost. *International Conference on Intelligent Environments (IE)* **2017**.
2. Ding, L.; Noborio, K.; Shibuya, K. Modelling and learning cause-effect—application in frost forecast. *Procedia Computer Science* **2020**, *176*, 2264–2273.
3. Diedrichs, A.L.; Bromberg, F.; Dujovne, D.; Brun-Laguna, K.; Watteyne, T. Prediction of frost events using machine learning and IoT sensing devices. *IEEE Internet of Things Journal* **2018**, *5*, 4589–4597.
4. Lira, H.; Martí, L.; Sanchez-Pi, N. Frost forecasting model using graph neural networks with spatio-temporal attention. AI: Modeling Oceans and Climate Change Workshop at ICLR 2021, 2021.
5. Hewage, P.; Trovati, M.; Pereira, E.; Behera, A. Deep learning-based effective fine-grained weather forecasting model. *Pattern Analysis and Applications* **2021**, *24*, 343–366.
6. Veličković, P.; Cucurull, G.; Casanova, A.; Romero, A.; Lio, P.; Bengio, Y. Graph attention networks. *arXiv preprint arXiv:1710.10903* **2017**.
7. Cheng, D.; Wang, X.; Zhang, Y.; Zhang, L. Graph Neural Network for Fraud Detection via Spatial-temporal Attention. *IEEE Transactions on Knowledge and Data Engineering* **2020**.
8. Shang, C.; Chen, J.; Bi, J. Discrete Graph Structure Learning for Forecasting Multiple Time Series. *arXiv preprint arXiv:2101.06861* **2021**.
9. Wu, Z.; Pan, S.; Long, G.; Jiang, J.; Chang, X.; Zhang, C. Connecting the dots: Multivariate time series forecasting with graph neural networks. Proceedings of the 26th ACM SIGKDD International Conference on Knowledge Discovery & Data Mining, 2020, pp. 753–763.
10. Mort, N.; Chia, C.L. Minimum temperature prediction in agricultural area using artificial neural networks. *IEE Colloquium on Neural Networks for Systems: Principles and Applications* **1991**.
11. Verdes, P.F.; Granitto, P.M.; Navone, H.D.; Ceccatto, H.A. Frost prediction with machine learning techniques. VI Congreso Argentino de Ciencias de la Computación, 2000.
12. Y Muck, P.; J Homam, M. Iot Based Weather Station Using Raspberry Pi 3. *International Journal of Engineering & Technology* **2018**.
13. Levin Varghese, Gerard Deepak, s.S.A. An IoT Analytics Approach for Weather Forecasting using Raspberry Pi 3 Model B+. *2019 Fifteenth International Conference on Information Processing (ICINPRO)* **2019**.
14. Castañeda-Miranda, A.; Castaño-Meneses, V.M. Internet of things for smart farming and frost intelligent control in greenhouses. *Computers and Electronics in Agriculture* **2020**, *176*, 105614.
15. Guillén-Navarro, M.A.; Martínez-España, R.; López, B.; Cecilia, J.M. A high-performance IoT solution to reduce frost damages in stone fruits. *Concurrency and Computation: Practice and Experience* **2021**, *33*, e5299.
16. Cadenas, J.M.; Garrido, M.; Martínez-España, R.; Guillén-Navarro, M.A. Making decisions for frost prediction in agricultural crops in a soft computing framework. *Computers and Electronics in Agriculture* **2020**, *175*, 105587.
17. Guillén-Navarro, M.A.; Martínez-España, R.; Llanes, A.; Bueno-Crespo, A.; Cecilia, J.M. A deep learning model to predict lower temperatures in agriculture. *Journal of Ambient Intelligence and Smart Environments* **2020**, *12*, 21–34.
18. Shi, X.; Chen, Z.; Wang, H.; Yeung, D.Y.; Wong, W.K.; Woo, W.C. Convolutional LSTM network: A machine learning approach for precipitation nowcasting. *Advances in neural information processing systems* **2015**, *2015*, 802–810.

19. Mehrkanoon, S. Deep shared representation learning for weather elements forecasting. *Knowledge-Based Systems* **2019**, *179*, 120–128.
20. Zhang, S.; Tong, H.; Xu, J.; Maciejewski, R. Graph convolutional networks: a comprehensive review. *Computational Social Networks* **2019**, *6*, 1–23.
21. Wilson, T.; Tan, P.N.; Luo, L. A Low Rank Weighted Graph Convolutional Approach to Weather Prediction. 2018 IEEE International Conference on Data Mining (ICDM). IEEE, 2018, pp. 627–636.
22. Khodayar, M.; Wang, J. Spatio-temporal graph deep neural network for short-term wind speed forecasting. *IEEE Transactions on Sustainable Energy* **2018**, *10*, 670–681.
23. Wang, S.; Li, Y.; Zhang, J.; Meng, Q.; Meng, L.; Gao, F. PM2.5-GNN: A Domain Knowledge Enhanced Graph Neural Network For PM2.5 Forecasting. Proceedings of the 28th International Conference on Advances in Geographic Information Systems, 2020, pp. 163–166.
24. Gao, J.; Sharma, R.; Qian, C.; Glass, L.M.; Spaeder, J.; Romberg, J.; Sun, J.; Xiao, C. STAN: spatio-temporal attention network for pandemic prediction using real-world evidence. *Journal of the American Medical Informatics Association* **2021**, *28*, 733–743.
25. Song, C.; Lin, Y.; Guo, S.; Wan, H. Spatial-temporal synchronous graph convolutional networks: A new framework for spatial-temporal network data forecasting. Proceedings of the AAAI Conference on Artificial Intelligence, 2020, Vol. 34, pp. 914–921.
26. Lu, Y.J.; Li, C.T. AGSTN: Learning Attention-adjusted Graph Spatio-Temporal Networks for Short-term Urban Sensor Value Forecasting. 2020 IEEE International Conference on Data Mining (ICDM). IEEE, 2020, pp. 1148–1153.
27. Kong, X.; Xing, W.; Wei, X.; Bao, P.; Zhang, J.; Lu, W. STGAT: Spatial-temporal graph attention networks for traffic flow forecasting. *IEEE Access* **2020**, *8*, 134363–134372.
28. Li, D.; Lasenby, J. Spatiotemporal Attention-Based Graph Convolution Network for Segment-Level Traffic Prediction. *IEEE Transactions on Intelligent Transportation Systems* **2021**.
29. Seo, Y.; Defferrard, M.; Vandergheynst, P.; Bresson, X. Structured sequence modeling with graph convolutional recurrent networks. International Conference on Neural Information Processing. Springer, 2018, pp. 362–373.
30. Yu, B.; Yin, H.; Zhu, Z. Spatio-temporal graph convolutional networks: A deep learning framework for traffic forecasting. *arXiv preprint arXiv:1709.04875* **2017**.
31. Zhao, L.; Song, Y.; Zhang, C.; Liu, Y.; Wang, P.; Lin, T.; Deng, M.; Li, H. T-GCN: A temporal graph convolutional network for traffic prediction. *IEEE Transactions on Intelligent Transportation Systems* **2019**, *21*, 3848–3858.
32. Sutskever, I.; Vinyals, O.; Le, Q.V. Sequence to sequence learning with neural networks. *arXiv preprint arXiv:1409.3215* **2014**.